Biosensors and Bioelectronics 45 (2013) 163–167

Contents lists available at SciVerse ScienceDirect

Biosensors and Bioelectronics

journal homepage: www.elsevier.com/locate/bios

Short communication

Detecting Lyme disease using antibody-functionalized single-walled carbon nanotube transistors

Mitchell B. Lerner [a,1], Jennifer Dailey [a,1], Brett R. Goldsmith [a,2], Dustin Brisson [b], A.T. Charlie Johnson [a,*]

[a] Department of Physics and Astronomy, University of Pennsylvania, 209 South 33rd Street, Philadelphia, PA 19104, USA
[b] Department of Biology, University of Pennsylvania, 3740 Hamilton Walk, Philadelphia, PA 19104, USA

ARTICLE INFO

Article history:
Received 17 October 2012
Received in revised form
13 January 2013
Accepted 21 January 2013
Available online 4 February 2013

Keywords:
Carbon nanotubes
Lyme
FET

ABSTRACT

We examined the potential of antibody-functionalized single-walled carbon nanotube (SWNT) field-effect transistors (FETs) to use as a fast and accurate sensor for a Lyme disease antigen. Biosensors were fabricated on oxidized silicon wafers using chemical vapor deposition grown carbon nanotubes that were functionalized using diazonium salts. Attachment of *Borrelia burgdorferi* (Lyme) flagellar antibodies to the nanotubes was verified by atomic force microscopy and electronic measurements. A reproducible shift in the turn-off voltage of the semiconducting SWNT FETs was seen upon incubation with *B. burgdorferi* flagellar antigen, indicative of the nanotube FET being locally gated by the residues of flagellar protein bound to the antibody. This sensor effectively detected antigen in buffer at concentrations as low as 1 ng/ml, and the response varied strongly over a concentration range coinciding with levels of clinical interest. Generalizable binding chemistry gives this biosensing platform the potential to be expanded to monitor other relevant antigens, enabling a multiple vector sensor for Lyme disease. The speed and sensitivity of this biosensor make it an ideal candidate for development as a medical diagnostic test.

1. Introduction

Lyme disease is a tick-borne illness caused by the bacteria *Borrelia burgdorferi*, generating at least 30,000 new cases in the United States each year, although there are likely many more cases that go undetected or misdiagnosed due to generality of symptoms (Centers for Disease Control and Prevention, 2011). Of the patients diagnosed with Lyme disease, many are originally misdiagnosed due to the general symptoms of the disease (Williams et al., 1990), inconsistent disease presentation in patients (Aguerorosenfeld et al., 1993), and lack of sensitive testing available for early stages of the infection (Bakken et al., 1997). Late detection of Lyme disease can result in further complications including arthritis and permanent neurological disorders (Marques, 2008). Diagnosis of Lyme disease is severely hindered by the lack of reliable diagnostic tools despite its importance to treatment success (Murray and Shapiro, 2010; O'Connell, 2010). A reliable and rapid laboratory diagnostic tool is crucial for reducing the number of misdiagnosed patients and for investigating appropriate treatment protocols for chronic Lyme disease.

In recent years, great progress has been made in the field of carbon nanotube field effect transistor (CNT FET)-based biosensors (Allen et al., 2007). Benefits of nanotube-based sensors include the speed and reliability obtained from performing multiple assays in parallel (Chikkaveeraiah et al., 2009). Protein-functionalized nanotube-based FETs are of great research and clinical interest for several reasons. Their nanometer size is comparable to the size of many biomolecules of interest, suggesting a unique biocompatible platform (Harrison and Atala, 2007; Lerner et al., 2011; Sudibya et al., 2009). Additionally, since every atom of a carbon nanotube is located on its surface, in direct contact with the environment, they are a clear choice for direct environmental sensing. Commercially available assays for Lyme-specific antigens in urine and cerebrospinal fluid have a limit of detection of 12–15 ng/mL (Shah et al., 2004). We hypothesized that an antibody-functionalized SWNT FET immunosensor would be able to detect the small amount of Lyme antigen that is present in bodily fluids at very early stages of Borrelia infection (Harris and Stephens, 1995) since protein-functionalized nano-enabled sensors have demonstrated very low detection limits, on the order of fM (Duan et al., 2012; Lerner et al., 2012a). Direct detection of the antigen provides

* Corresponding author. Tel.: +1 2158989325
E-mail address: cjohnson@physics.upenn.edu (A.T. Charlie Johnson).
[1] These authors contributed equally to this work.
[2] Current address: SPAWAR Systems Center Pacific, 53560 Hull Street, San Diego, CA 92152, USA.

0956-5663/$ - see front matter © 2013 Elsevier B.V. All rights reserved.
http://dx.doi.org/10.1016/j.bios.2013.01.035

earlier test results because it eliminates the delay required for the immune system to produce sufficient quantities of antibodies to be detected via Western Blot or ELISA, which can improve patient prognosis (Ma et al., 1992). Here we demonstrate that antibody-functionalized SWNT FET devices are effective biosensors for rapidly detecting Lyme flagellar antigen at clinically relevant concentrations, as low as 1 ng/ml, with negligible response to negative-control proteins and to pure buffer solution.

2. Materials and methods

2.1. Device fabrication

Carbon nanotube transistors were fabricated using previously described methods (Goldsmith et al., 2011; Khamis et al., 2011). Briefly, a solution of iron (III) nitrate dissolved in isopropanol was spin coated onto a p^{2+} doped Si/SiO_2 wafer to give an iron catalyst layer. Single-walled carbon nanotubes were grown by catalytic chemical vapor deposition (CVD) with methane (2500 sccm) as the carbon source in a background of forming gas (600 sccm Ar, 320 sccm H_2) at 900 °C for 2 min. Following the growth, an optimized bilayer photolithography process using PMGI and Shipley 1813 (Khamis et al., 2011) was used to pattern source and drain electrodes with 2.5 μm channel length that were then metallized (3 nm Ti/40 nm Pd) using thermal evaporation. The doped silicon substrate served as a global backgate to complete the three terminal field-effect transistor geometry. Devices were individually characterized by sweeping the back gate voltage from −10 V to 10 V while holding the bias voltage fixed at 100 mV. Approximately 80 high quality semiconducting SWNT devices with ON/OFF ratios >1000 were selected to use in experiments.

2.2. Protein functionalization

Monoclonal Lyme antibodies specific for *B. Burgdorferi* flagellar antigen (p41) were obtained commercially (antibodies-online.com). Histidine-tagged Lyme antigen containing the p41 flagellar immunodominant region (also known as flagellin) was obtained from ProSpec. Antigen was diluted with Tris–HCl buffer (pH 7.5), aliquoted to several concentrations and stored at 4 °C. Antibodies were aliquoted at a concentration of 1 μg/ml in Tris–HCl buffer and stored at −20 °C.

Nanotube functionalization followed previously documented procedures (Goldsmith et al., 2011; Lerner et al., 2012a) adapted from (Strano et al., 2003) (see Fig. 1). Carbon nanotubes were functionalized using diazonium salts synthesized according to a published recipe (Saby et al., 1997). Samples were immersed in a solution of 4-carboxybenzene diazonium tetrafluoroborate at a concentration of 2.5 mg/1 mL deionized (DI) water for 1 h at 40 °C to create sp^3 hybridization sites ending in carboxylic acid groups, then rinsed for 1 min each in acetone, methanol, and deionized water baths. The carboxylic acid groups were then activated with EDC and stabilized with sulfo-NHS at concentrations of 6 mg and 16 mg per 15 mL MES buffer (pH 6.0) respectively for 15 min at room temperature, followed by a DI water rinse. A solution of antibodies at a concentration of 1 μg/mL was pipetted onto the nanotube devices in a humid environment to prevent the solution from evaporating, causing primary amines on the antibody to displace stabilized sulfo-NHS sites over a period of 1 h. The devices were washed thoroughly by rinsing in two DI water baths for 2 min each and dried with gentle (less than 20 psi) nitrogen flow in order to minimize the amount of salts and non-specifically bound proteins on the device.

Antibody-functionalized SWNT-FET devices were similarly exposed to droplets of antigen at a known concentration for 20 min in a humid environment to prevent the droplet from evaporating. Exposure to Lyme flagellar antigen occurred over a sufficiently long time for the proteins to diffuse to the sensor and establish equilibrium between bound and unbound species. This is known to be a critical consideration for detection of biomolecular analytes at pM or lower concentration (Squires et al., 2008). The devices were then washed in two DI water baths for 2 min each to remove non-specifically bound antigen and dried with gentle nitrogen flow. Each device was exposed to only one concentration of antigen in order to avoid contamination of samples, and each concentration of antigen was tested on 5–10 functionalized devices to ensure reproducibility of the results.

3. Results and discussion

In order to verify the validity of the attachment chemistry, Atomic Force Microscopy (AFM) data were gathered on an Asylum AFM in tapping mode followed by both antibody attachment (Fig. 2a) and subsequent exposure to flagellar antigen at a concentration of 400 ng/mL (Fig. 2b). Fig. 2a (Fig. 2b) is an AFM image showing small ball-like features that are associated with bound antibodies (antibody/antigen complexes), with a density ca. 3-5 attachments per micrometer. As is typically found in AFM analysis, the lateral dimension of the features (~50 nm in Fig. 2b) is larger than the molecular size, which is an artifact associated with the finite radius of the AFM tip. The *height* of the features is therefore compared with the expected size of the antibody and antibody/antigen complex. Statistical analysis of the feature heights in Fig. 2a shows that the antibodies are 2.78 nm ± 0.22 nm in size, slightly smaller than expected for a complete IgG. This is likely due to the protein being slightly distorted during the tapping mode AFM in air, as we have reported previously (Johnson et al., 2009; Zhang et al., 2007). After exposure to flagellar antigen, the histogram of feature heights shows new peaks at 4.7 ± 0.6 nm and 6.5 ± 0.4 nm associated with larger antibody/antigen complexes. These are ascribed to binding of one and two antigen proteins, respectively, to a bound antibody, consistent with the fact that the IgG used in the experiments has two binding sites (Talwar and Srivastava, 2006). Each added antigen increases the feature height by ~1.8 nm. There also appears to be an additional minor peak at ~3 nm that represents unreacted antibodies; this peak accounts for ~20% of the total features measured. These data suggest that after exposure to antigen at 400 ng/mL, approximately 80% of the antibodies have bound to at least one antigen, in good agreement with the electronic response data presented in Fig. 3b.

We conducted a control experiment to establish that nanotubes and the nanotube/SiO_2 interface show very low affinity for non-specific binding of the Lyme antigen; details are provided in Supplementary material Fig. S1. When as-prepared nanotube devices were exposed to a high concentration (1 μg/mL) of Lyme antigen, there was minimal non-specific binding to the nanotubes or to the surrounding substrate. We also confirmed that exposure to the Lyme antigen at this concentration had negligible effect on the electronic characteristics of the device. These control experiments provide strong evidence that the biosensor responses described below reflect specific binding of the antigen.

Electronic measurements of the current as a function of the backgate voltage (I–V_g characteristics) for individual NT FET devices were taken following each chemical modification to monitor the effect of chemical functionalization and to confirm attachment of antibodies (Fig. 3a). Parameters of interest included I_{ON}, the ON state current of the device, and V_{TH}, the threshold voltage, where the line tangent to the I–V_g curve intersects the gate voltage axis. A 50–90% drop in I_{ON} as well as a 3–4 V decrease in

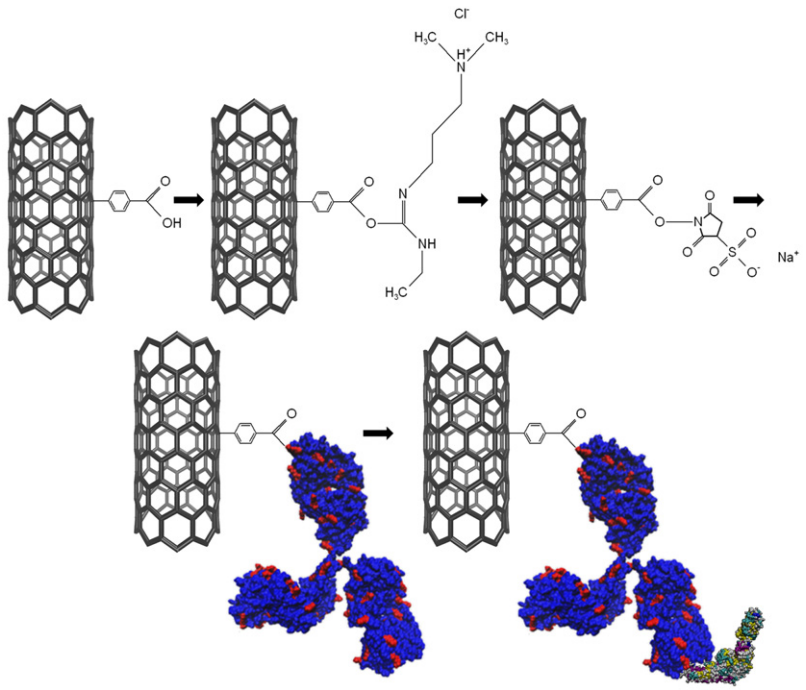

Fig. 1. Functionalization chemistry for Lyme antibody and binding of flagellar antigen. First, a pristine nanotube is treated with diazonium salts to create sp^3 hybridization sites ending in carboxylic acid moieties. The carboxylic acid is activated with EDC and stabilized with sulfo-NHS. The sulfo-NHS is displaced by the primary amine in a surface lysine residue (depicted in red) on the anti-p41 antibody. The flagellar antigen (depicted according to secondary structure in purple, cyan, and yellow) then binds to the epitope on the antibody during the exposure step. (For interpretation of the references to color in this figure legend, the reader is referred to the web version of this article.)

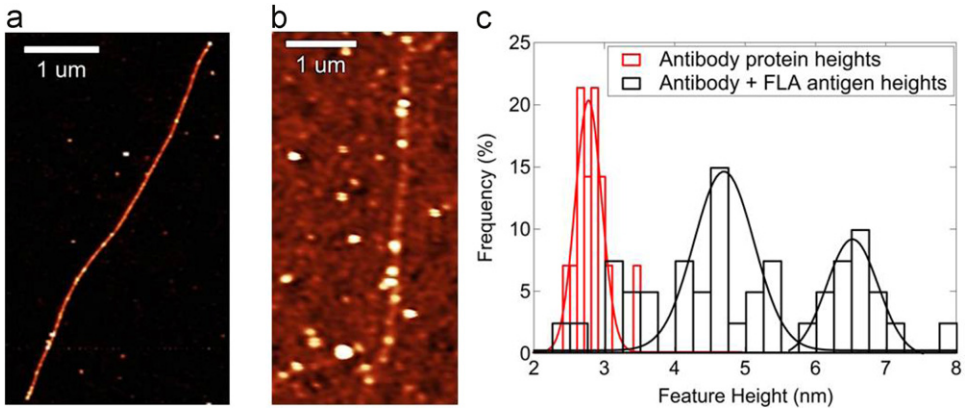

Fig. 2. (a) AFM image of anti-p41 antibody proteins attached to carbon nanotubes. *Z* scale is 6 nm, average protein feature is ~2.8 nm in size. (b) AFM image after incubation in a solution of FLA antigen at a concentration of 400 ng/mL shows antigen attached to bound antibodies on a nanotube. *Z* scale is 8 nm. (c) Histogram of feature heights following antibody attachment (red data) and exposure to antigen (black data). (For interpretation of the references to color in this figure legend, the reader is referred to the web version of this article.)

the threshold voltage resulted from diazonium oxidation, which is associated with the creation of sp^3 hybridization sites terminated with a carboxylic acid group. EDC/NHS treatment resulted in a slight decrease in the ON state current, while the change in the threshold voltage varied from sample to sample (e.g., V_{TH} shows a decrease in Fig. 3a and an increase in Fig S2 of the Supplemental material). The reason for this variation remains a subject for future research. Following antibody attachment, there was typically an increase in ON state current, suggesting that the attachment led to a decrease in carrier scattering. Upon antigen exposure, a shift in the threshold voltage toward more negative values was consistently observed. There was no statistically significant change in ON state current following antigen exposure.

There was a systematic dependence of the threshold voltage shift with varying antigen concentration in the range from 0.1 ng/ml to 3 μg/ml, with each concentration tested on 5–10 functionalized devices. The variation of the average measured shift in the threshold voltage as a function of antigen concentration is displayed in Fig. 3b. Error bars shown are the standard error of the mean. The sensor responses agree with a model based on the Hill–Langmuir equation for equilibrium protein binding (see Fig. 3b) (Hill, 1910; Lehninger et al., 2008):

$$\Delta V_{TH} = A\frac{(c/K_d)^n}{1+(c/K_d)^n} + Z$$

here c is the Lyme antigen concentration, A is the sensor response at saturation when all binding sites are occupied, Z is an overall offset to account for the response to pure buffer, K_d is the dissociation constant describing the concentration at which half

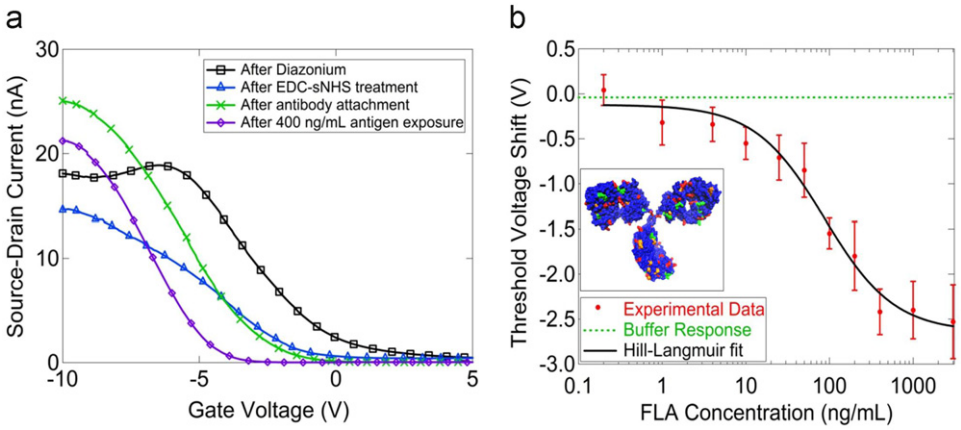

Fig. 3. (a) Current vs. gate voltage characteristics at subsequent stages of nanotube functionalization. The sensing response is 2.3 V decrease of the threshold voltage upon exposure to antigen (curve with green x to curve with purple diamond). (b) Threshold voltage shift as a function of antigen concentration can be fit with a model based on the Hill–Langmuir equation. These data indicate a limit of detection of ~1 ng/mL and non-cooperative antigen binding. Inset shows structure of anti-p41 Borrelia antibody with lysine (red), histidine (orange) and arginine (green) residues highlighted. Any of these basic residues could become protonated and generate a local gating effect if they come into closer contact with the nanotube upon antigen binding. (For interpretation of the references to color in this figure legend, the reader is referred to the web version of this article.)

of available binding sites are occupied, and n is the Hill coefficient describing cooperativity of binding.

The best fit to the data yielded a maximum response $A=-2.52\ \text{V}\pm0.32\ \text{V}$, offset parameter $Z=-0.12\ \text{V}\pm0.16\ \text{V}$, dissociation constant $K_d=87\ \text{ng/mL}\ \pm27\ \text{ng/mL}$, and $n=1.04\pm0.08$. The best fit value of the offset parameter $Z=-0.12\ \text{V}\ \pm0.16\ \text{V}$ was statistically indistinguishable from the experimentally measured responses of seven devices to pure buffer as a negative control ($\Delta V=0.11\ \text{V}\ \pm0.15\ \text{V}$). The value of $K_d=87\pm27\ \text{ng/mL}$ determined from the fit describes the concentration of antigen at which half the receptors are occupied; this regime coincides with antigen levels of diagnostic significance, 12–15 ng/mL (Shah et al., 2004). It is notable that the AFM image in Fig. 2b, taken after exposure to antigen at 400 ng/mL, shows occupation at ~80% of the attached antibody sites, in good agreement with the prediction of the Hill–Langmuir fit, that 95% of the active sites were occupied at this concentration. The slight discrepancy could be due to antibodies that were bound to the nanotube in such an orientation that their epitope is obstructed or otherwise non-functional. The Hill–Langmuir model combined with the AFM data suggested that the number of such antibodies unavailable for binding is no more than 20% of the total bound antibodies.

The best fit value of the cooperativity parameter, $n=1.04\pm0.08$, indicates independent binding of Lyme antigen to the anti-p41 in the context of the NT-FET biosensor. The data presented in Fig. 3b show that the measured responses from a collection of 5–10 devices could be used to differentiate between pure buffer solution ($\Delta V=0.11\ \text{V}\ \pm0.15\ \text{V}$) and buffer containing Lyme antigen at a concentration of 1 ng/mL ($\Delta V=-0.31\ \text{V}\ \pm0.24\ \text{V}$). Previous work suggests that this limit of detection may be lowered by as much as a factor of 1000 by replacing the complete IgG with its single chain variable fragment, thus allowing the binding event to occur closer to the nanotube where the electrostatic influence on transport in the NT transistor will be more pronounced (Lerner et al., 2012a). Although significant device-to-device variation was observed (as reflected in the error bars in Fig. 4), in this application the main concern is the detection of Lyme antigen at any level, rather than accurate measurement of its concentration. The results obtained in this experiment suggest that nanotube biosensors offer great promise for development into a useful diagnostic test.

The observed reduction in turnoff voltage is consistent with a gating effect due to the presence of positive charges in the local electrostatic environment of the carbon nanotube (Heller et al. 2008). The proposed mechanism responsible for introducing these positive local charges is a conformational change in the antibody protein upon binding the flagellar antigen, which results in the carbon nanotube being exposed to different amino acids on the antibody exterior. Charges in close proximity to carbon nanotubes have been shown to shift the transistor threshold voltage by local gating (Lerner et al., 2012b). Lysine, histidine, and arginine (highlighted in the inset of Fig. 3b) are common amino acids, a portion of which will be protonated when the pH is less than 7 and are thus candidates for locally gating the nanotube as observed. Experimental conditions may be as low as pH 5 due to deprotonation of silanol groups in a thin water layer that forms on the hydrophilic SiO_2 surface (Lerner et al., 2012b; O'Reilly et al., 2005). Even in the absence of a quantitative understanding of the device response, the results provide strong evidence that the methods used here enabled attachment of antibody proteins to a NT-FET while maintaining both the high quality electronic characteristics of the NT device and the chemical recognition functionality characteristic of the protein.

As a further control experiment, antibody-functionalized sensors were incubated in a solution of bovine serum albumin (BSA) at high concentration (1 μg/mL) to approximate the effect of non-specific proteins present in patient samples (human serum albumin is a large component of blood plasma proteins and represents a potential interfering agent; Peters, 1996). A sample I–V_g characteristic is presented in Supplementary material Fig. S2. The sensor response to BSA, averaged over eight devices, was a shift of $-0.13\ \text{V}\ \pm0.18\ \text{V}$, similar to the response produced by buffer alone. We thus concluded that the Lyme flagellar antibody-functionalized carbon nanotube transistors exhibited a high level of specificity for the flagellar protein target antigen.

4. Conclusions

We demonstrated that antibody-functionalized SWNT FET devices are effective biosensors for rapidly detecting Lyme disease antigen at diagnostically relevant concentrations. The sensor responses were rapid (minutes) and exhibited good reproducibility. We achieved detection of flagellar antigen protein at a concentration of 1 ng/ml with negligible response to control proteins and to pure buffer solution. The experiments showed an

antigen-specific, concentration-dependent sensor response over a wide range of concentrations (from 1 ng/mL to 3000 ng/mL) that was in excellent quantitative agreement with a model based on the Hill–Langmuir equation of equilibrium thermodynamics. Future work includes functionalizing samples with single chain variable fragments to increase sensitivity and the use of a sensor array based on multiple antibodies in order to capture several types of proteins indicative of Lyme disease for a multiplexed biosensor platform. The rapidity and ease of use of this sensor is superior to traditional immunoassays, suggesting its utility as a point-of-care diagnostic tool.

Acknowledgments

This research was supported by the Department of Defense US Army Medical Research and Materiel Command through Grants W81XWH-09-1-0205 and W81XWH-09-1-0206 (M.L., J.D. A.T.C.J.) and by the National Institutes of Health Grant R01AI076342 (D.B.). We acknowledge use of facilities associated with the Nano/Bio Interface Center, National Science Foundation NSEC DMR08-32802. J.D. acknowledges support of the REU program of the Laboratory for Research on the Structure of Matter (NSF REU Site Grant DMR-1062638) and of the Penn University Scholars program.

Appendix A. Supporting information

Supplementary data associated with this article can be found in the online version at http://dx.doi.org/10.1016/j.bios.2013.01.035.

References

Aguerorosenfeld, M.E., Nowakowski, J., Mckenna, D.F., Carbonaro, C.A., Wormser, G.P., 1993. Journal of Clinical Microbiology 31 (12), 3090–3095.
Allen, B.L., Kichambare, P.D., Star, A., 2007. Advanced Materials 19 (11), 1439–1451.
Bakken, L.L., Callister, S.M., Wand, P.J., Schell, R.F., 1997. Journal of Clinical Microbiology 35 (3), 537–543.
Centers for Disease Control and Prevention, 2011. N.C.f.E.a.Z.I.D.N., Division of Vector-Borne Diseases (DVBD), Lyme Disease: A Public Information Guide.
Chikkaveeraiah, B.V., Bhirde, A., Malhotra, R., Patel, V., Gutkind, J.S., Rusling, J.F., 2009. Analytical Chemistry 81 (21), 9129–9134.
Duan, X.X., Li, Y., Rajan, N.K., Routenberg, D.A., Modis, Y., Reed, M.A., 2012. Nature Nanotechnology 7 (6), 401–407.
Goldsmith, B.R., Mitala, J.J., Josue, J., Castro, A., Lerner, M.B., Bayburt, T.H., Khamis, S.M., Jones, R.A., Brand, J.G., Sligar, S.G., Luetje, C.W., Gelperin, A., Rhodes, P.A., Discher, B., Johnson, A.T.C., 2011. ACS Nano 5, 5408–5416.
Harris, N., Stephens, B.G., 1995. Journal of Spirochetal and Tick-borne Diseases 2, 37–41.
Harrison, B.S., Atala, A., 2007. Biomaterials 28 (2), 344–353.
Heller, I., Janssens, A.M., Mannik, J., Minot, E.D., Lemay, S.G., Dekker, C., 2008. Nano Letters 8 (2), 591–595.
Hill, A., 1910. Journal of Physiology 40, 4–7.
Johnson, R.R., Rego, B.L., Johnson, A.T.C., Klein, M.L., 2009. Journal of Physical Chemistry B 113, 11589–11593.
Khamis, S.M., Jones, R.A., Johnson, A.T.C., 2011. AIP Advances 1, 022106.
Lehninger, A.L., Nelson, D.L., Cox, M.M., 2008. Lehninger Principles of Biochemistry, 5th ed. W.H. Freeman, New York.
Lerner, M.B., D'Souza, J., Pazina, T., Dailey, J., Goldsmith, B.R., Robinson, M.K., Johnson, A.T.C., 2012a. ACS Nano 6 (6), 5143–5149.
Lerner, M.B., Goldsmith, B.R., McMillon, R., Dailey, J., Pillai, S., Singh, S.R., Johnson, A.T.C., 2011. AIP Advances 1, 042127.
Lerner, M.B., Resczenski, J.M., Amin, A., Johnson, R.R., Goldsmith, J.I., Johnson, A.T., 2012b. Journal of the American Chemical Society 134 (35), 14318–14321.
Ma, B., Christen, B., Leung, D., Vigo-Pelfrey, C., 1992. Journal of Clinical Microbiology 30 (2), 370–376.
Marques, A., 2008. Infectious Disease Clinics of North America 22 (2), 341–360 vii–viii.
Murray, T.S., Shapiro, E.D., 2010. Clinics in Laboratory Medicine 30 (1), 311–328.
O'Connell, S., 2010. Current Opinion in Infectious Diseases 23 3, 231–235.
O'Reilly, J.P., Butts, C.P., I'Anson, I.A., Shaw, A.M., 2005. Journal of the American Chemical Society 127 (6), 1632–1633.
Peters, T., 1996. All About Albumin: Biochemistry, Genetics, and Medical Applications. Academic Press, San Diego.
Saby, C., Ortiz, B., Champagne, G.Y., Belanger, D., 1997. Langmuir 13 (25), 6805–6813.
Shah, J., Harris, N., Bai, H., Remollo, G., 2004. Assay for Detection of Antigen in Bodily Fluid. In: Office, U.S.P.A.T. (Ed.). IGeneX, Inc., Palo Alto, CA, United States of America.
Squires, T.M., Messinger, R.J., Manalis, S.R., 2008. Nature Biotechnology 26 (4), 417–426.
Strano, M.S., Dyke, C.A., Usrey, M.L., Barone, P.W., Allen, M.J., Shan, H.W., Kittrell, C., Hauge, R.H., Tour, J.M., Smalley, R.E., 2003. Science 301 (5639), 1519–1522.
Sudibya, H.G., Ma, J.M., Dong, X.C., Ng, S., Li, L.J., Liu, X.W., Chen, P., 2009. Angewandte Chemie International Edition 48 (15), 2723–2726.
Talwar, G.P., Srivastava, L.M., 2006. Textbook of Biochemistry and Human Biology, 3rd ed. Prentice-Hall of India Private Limited, New Delhi, India.
Williams, C.L., Strobino, B., Lee, A., Curran, A.S., Benach, J.L., Inamdar, S., Cristofaro, R., 1990. The Pediatric Infectious Disease Journal 9 (1), 10–14.
Zhang, Y.B., Kanungo, M., Ho, A.J., Freimuth, P., van der Lelie, D., Chen, M., Khamis, S.M., Datta, S.S., Johnson, A.T.C., Misewich, J.A., Wong, S.S., 2007. Nano Letters 7 (10), 3086–3091.